

Investigation of Glass-to-Concrete Adhesive Joints through Three-Point Bending Tests

Cas Maertens ^a, Bert Van Lancker ^{b,c}, Alessandro Proia ^b, Roman Wan-Wendner ^b, Jan Belis ^b

a Ghent University, Belgium, cas.maertens@ugent.be

b Ghent University, Belgium

c Vitroplena, Belgium

Abstract

This study aims to explore innovative structural applications involving the bonding of glass to concrete. To date, academic literature has provided limited insights into the adhesive bonding between glass and concrete. This investigation focuses on understanding the bond behaviour of glass-concrete joints through small-scale three-point bending tests. The analysis shows how variations in the adhesive joint configuration and the selection of adhesives impacts the bond behaviour. By systematically examining these factors, the aim is to provide valuable insights into optimising the design and construction of bonded glass-concrete elements. These insights serve as the foundation for future studies, exploring innovative applications where structural considerations seamlessly merge with aesthetic, durability, and safety considerations. The ultimate objective is to evaluate the potential of glass bonded to concrete, aiming to not only excel in structural performance but also to meet multifaceted demands across diverse engineering applications.

Keywords

Glass, Concrete, Adhesive, Glass-to concrete joint, Bonding, Three-point bending test

Article Information

- Digital Object Identifier (DOI): [10.47982/cgc.9.561](https://doi.org/10.47982/cgc.9.561)
- Published by [Challenging Glass](#), on behalf of the author(s), at [Stichting OpenAccess](#).
- Published as part of the peer-reviewed [Challenging Glass Conference Proceedings](#), Volume 9, June 2024, [10.47982/cgc.9](https://doi.org/10.47982/cgc.9)
- Editors: Christian Louter, Freek Bos & Jan Belis
- This work is licensed under a [Creative Commons Attribution 4.0 International](#) (CC BY 4.0) license.
- Copyright © 2024 with the author(s)

1. Introduction

In the last decades, significant advancement in the structural use of glass has emerged (Serafinavičius & Kvedaras, 2011). A major reason for this is the unique combination of properties which make glass a very attractive building material. Next to transparency, glass has a high compressive strength, a relatively high tensile strength, and a very good durability, recyclability, and resistance to environmental factors (Achintha, 2016; Narayanasamy et al., 2018; Udi et al., 2023). Initially, glass panes served primarily to fill load-bearing window frames. However, today, glass has evolved into a primary construction material for various architectural elements including glass facades, load-bearing structures such as columns and beams, as well as floor slabs and stiffening fins of facades.

In certain applications, the use of glass opens up possibilities regarding durability, safety, aesthetics, etc. Glass is inherently more resistant to aggressive environmental factors, such as moisture, chemicals, and UV radiation, compared to other materials (Popovici & Lupascu, 2012). Also, transparency is frequently a key consideration when using glass, and this characteristic opens up a unique perspective for its application in conjunction with concrete. Using adhesives to bond glass to concrete has a significant impact on the visual aspect of the element. There are no visible fasteners, so design possibilities become cleaner and more visually pleasing, enhancing the overall aesthetics of structures or architectural elements. Additionally, avoiding local fixings such as bolts reduces the occurrence of local stress peaks (Centelles et al., 2018). Fig. 1. displays a hybrid glass-concrete beam, where glass is structurally activated as web of the element (Freytag, 2004).

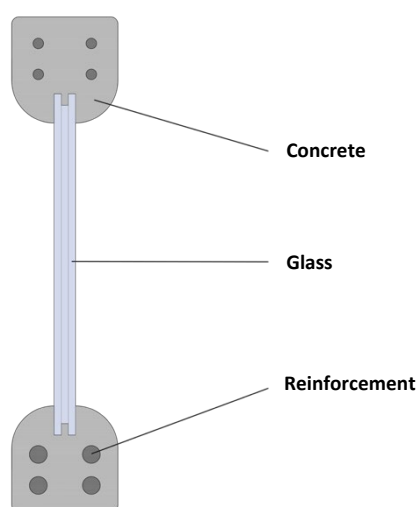


Fig. 1: Glass-concrete hybrid glass beam, based on Freytag (2004).

Traditionally, reinforced concrete structures rely on internal steel rebars to augment their bearing capacity to external loads. The high tensile strength, ductility, thermal compatibility, well-defined yield point, modulus of elasticity, and fatigue resistance make steel a suitable material for concrete reinforcement. However, steel is susceptible to corrosion in aggressive environments, leading to degradation and compromising the integrity of reinforced concrete elements over time (Lee & Cho, 2009).

A possible alternative is the use of Fiber Reinforced Polymer (FRP) as internal reinforcement and for strengthening applications. Overall, FRP shows several advantages such as corrosion resistance, high strength-to-weight ratio, and ease of installation compared to traditional steel reinforcement. However, FRP is vulnerable to temperature fluctuations, which can cause expansion and contraction, potentially leading to delamination or debonding from the concrete matrix. Additionally, FRP materials can be sensitive to UV radiation, which may degrade the polymers over time, reducing their effectiveness as reinforcement. Moreover, externally bonded FRP is often visually less attractive. Furthermore, the long-term durability and performance of FRP materials in concrete structures are still being studied and are not as well-established as those of traditional steel reinforcement (Tatar & Milev, 2021).

Glass might also be an interesting material to use in combination with concrete. Crushed glass can be used as coarse aggregate to produce more sustainable concrete (Sharma et al., 2022; Harrison, 2020). However, the aim is to explore a more high-grade application of glass in conjunction with concrete that leverages its strengths while acknowledging its limitations. In this study, we focus on the potential of using glass as an externally bonded stiffener, recognizing that while glass may not replace steel reinforcement for load-bearing purposes, it can serve as an additional stiffening element, particularly enhancing the structural performance in the serviceability limit state (SLS). By attaching a glass plate to the tension side of a concrete element, structural enhancement may be achieved, contributing to improved deflection control and crack mitigation in SLS conditions. The paper specifically investigates the ability of the glass-concrete joint to transfer loads and its implications for enhancing the structural behaviour under service loads.

In addition, although not the main focus of the study, there might be some advantages also in ULS design. For instance, following the standard NBN EN 1992-1-1 (Eurocode 2, 2005) concrete with a strength class of C20/25 has a characteristic axial tensile strength of 1.5 MPa. According to CEN/TS 19100-1:2021 (Design of glass structures, 2021), basic soda lime silica glass has a characteristic bending strength of 45 MPa. It is well known that by pre-stressing soda lime silica glass, higher values can be reached. In detail, the characteristic bending strengths of heat strengthened, thermally toughened, and chemically strengthened glass are, according to the standard, respectively 70 MPa, 120 MPa and 150 MPa. This makes that the tensile strength of glass is around 10-30% of that of standard rebar steel (BE500S).

The focus of this study is to investigate the bond behaviour of glass-concrete joints in structural engineering. Through three-point bending tests on small scale concrete specimens, this research examines how the adhesive joint configuration and the type of adhesive influence the structural performance of the hybrid elements. For each test the failure mode, glass stress and stiffness are examined. These insights serve as the foundation for future studies, exploring innovative applications where structural considerations merge with aesthetic, durability, and safety considerations. The ultimate objective is to evaluate the potential of glass bonded to concrete, aiming to not only excel in structural performance but also to meet multifaceted demands across diverse engineering applications.

2. Materials and methods

2.1. Specimen design

As there is no standard for glass-to-concrete adhesive bonds, the standard for FRP composite bonded to concrete (ASTM D7958/D7958M) is taken as a reference for the design of the specimens and the calculations.

The concrete prisms have nominal dimensions: 600 mm length (L) x 150 mm width (b) x 150 mm depth (d). There is a notch that covers half of the beam's height and impedes the concrete's ability to withstand tensile forces. A glass plate (200 mm x 125 mm x 8 mm) is bonded to the concrete using a structural adhesive. Due to the glass-concrete bonding, shear stresses between the glass plate and the concrete substrate are transferred until the debonding process is complete. As the notch opens up when the sample is loaded in a 3-point bending test, the adhesive undergoes shear and possibly also peel stresses, leading to tensile stresses in the glass.

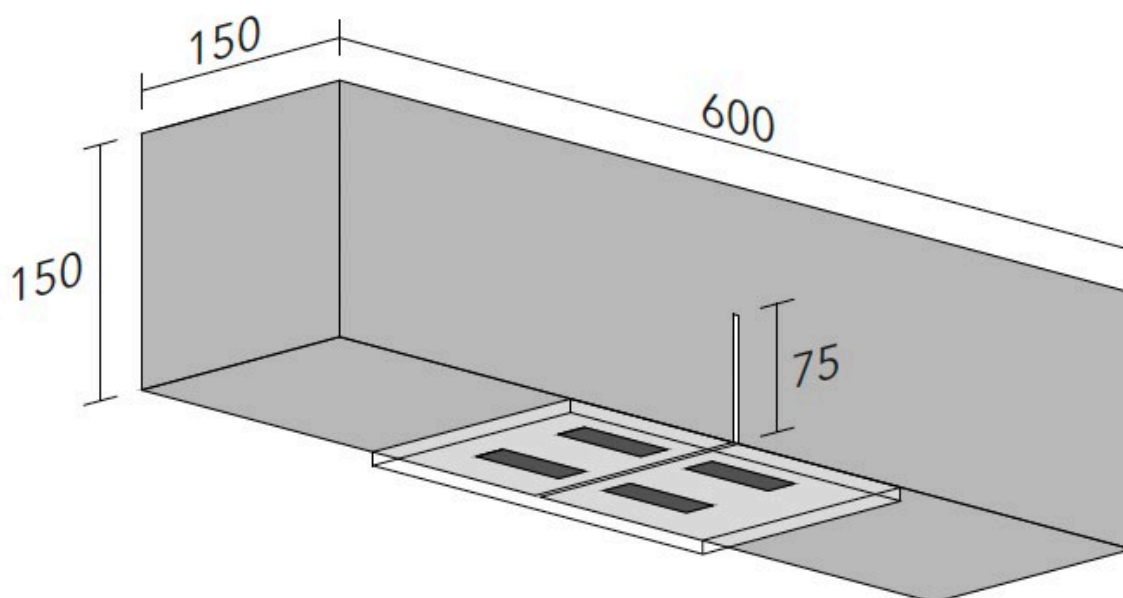


Fig. 2: Schematic drawing of the tested samples.

To investigate the influence of the adhesive joint configuration, three different configurations with five specimens each are tested. Each specimen has a total bond area of 5000 mm² (see Fig. 3). In the first configuration, the adhesion area is placed close and parallel to the notch. The bond length is 20 mm, and there is a debonded region of 20 mm from the notch. Adhesive joint configuration 2 consists of two adhesion strips on each side perpendicular to the notch but keeping distance with the edges of the glass (20 mm) and the notch (15 mm). The third configuration also has two strips on each side, but the strips cover the whole length from the notch to the glass edge. The bond length is 98 mm, and there is no debonded region. The adhesive thickness is 0.5 mm.

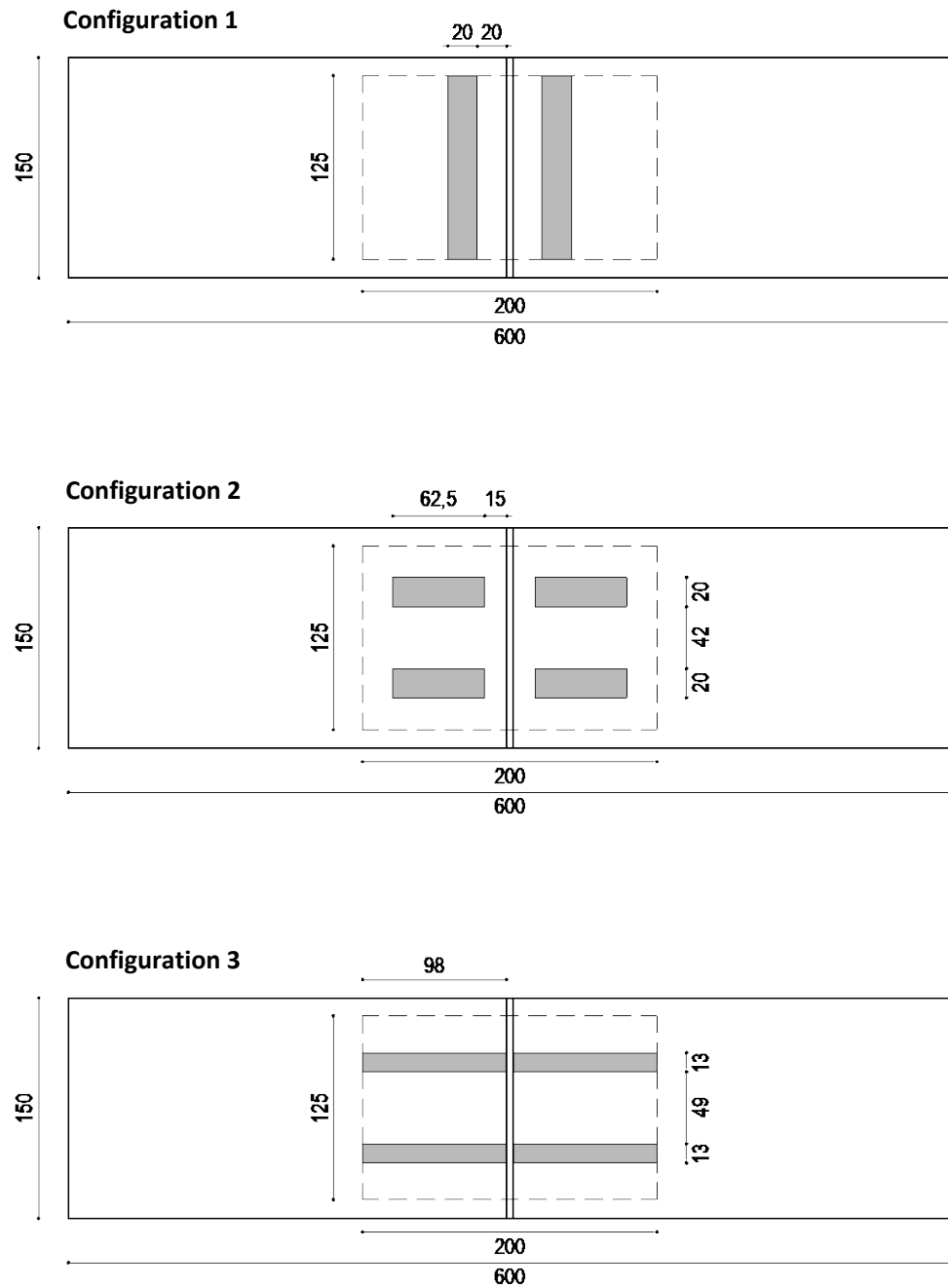


Fig. 3: Adhesive joint configurations 1, 2 and 3.

2.2. Materials

To determine the concrete compressive strength, three concrete cylinders with a size of 150 mm diameter and 300 mm height have been tested in compression after 28 days of curing. The average compressive strength was 30 MPa.

Basic soda lime silica glass without edge finishing is used. According to the glass standards (Design of glass structures, 2021), basic soda lime silica glass has a characteristic bending strength of 45 MPa.

Four different adhesives are used in the tests (see Table 1). Adhesive E is an epoxy-based adhesive, adhesive A is an acrylate-based adhesive, adhesive EM is an epoxy-based injection mortar and adhesive HP is a hybrid polymer-based adhesive.

Adhesive E is used to investigate the influence of the adhesive joint configuration. Next to that, all four adhesives are tested with joint configuration 3, to investigate the influence of the adhesive type.

Table 1: Adhesives.

Adhesive label	Adhesive type	Tested joint configuration(s)
Adhesive E	Epoxy-based adhesive	1, 2, 3
Adhesive A	Acrylate-based adhesive	3
Adhesive EM	Epoxy-based injection mortar	3
Adhesive HP	Hybrid polymer-based adhesive	3

2.3. Installation process

After the notch in the concrete samples was made, the samples are cleaned using pressurised air to remove the dust. Subsequently, an adhesive is applied onto the concrete using a PVC sheet as a mould. Prior to bonding, the glass plates are cleaned using acetone. Finally, the glass is positioned with its air side facing towards the adhesive.

After the adhesive is applied, the sample is placed in a room with a constant temperature (23 °C) and relative humidity (50%) for at least the number of days as prescribed in the technical data sheet of the adhesive.

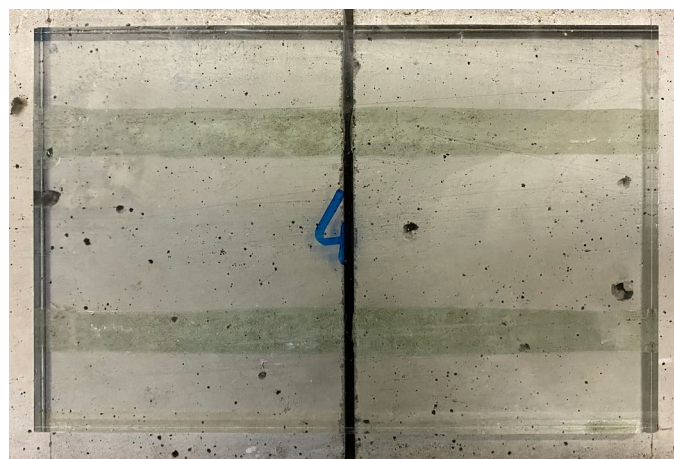


Fig. 4: Specimen with adhesive A.

2.4. Test setup

The 3-point bending tests, with a span of 500 mm, are performed using a Universal Test Machine (UTM) with a load cell of 100 kN. The accuracy of the load cell is 0,01%. The test is displacement controlled, using a test rate of 0.5 mm/min. Fig. 5 displays the test setup of a specimen with adhesive joint configuration 3.



Fig. 5. Test setup.

3. Results and discussion

3.1. Influence of adhesive joint configuration

For each test, the results are reported in the form of a load-displacement curve (see Fig. 6). The vertical displacement in mm measured by the UTM is reported on the x-axis; the applied load is shown on the y-axis.

According to the test results, the mean maximum force at failure was calculated, accompanied by the corresponding coefficient of variation. The test result of each adhesive configuration is reported (see Table 2), followed by a discussion and reflection.

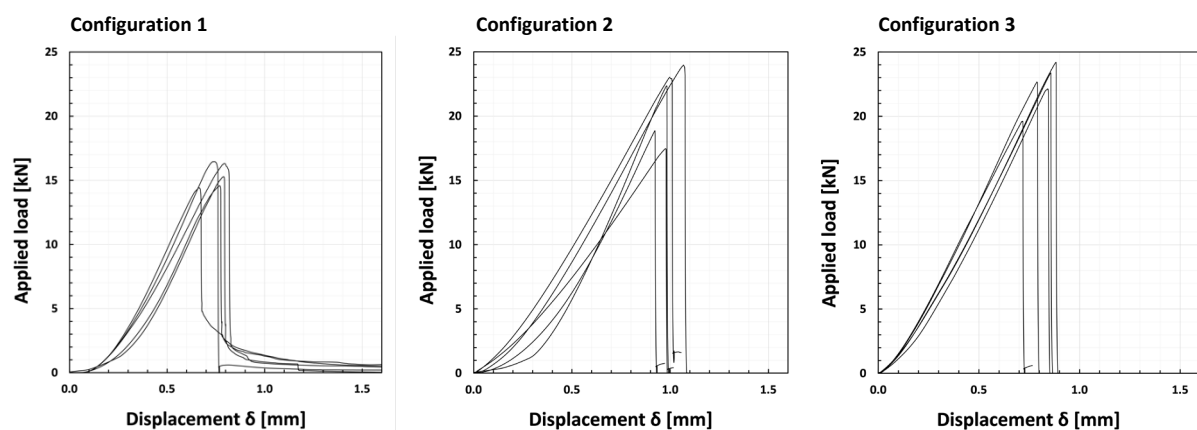


Fig. 6: Load-displacement curves of the reference beam and the specimens with adhesive joint configurations 1 , 2 and 3.

Table 2: Summarising table of the test results.

Configuration	Mean maximum load (kN)	Standard deviation (kN)	COV (%)
1	15.4	0.9	5.5
2	21.1	2.5	11.9
3	22.4	1.6	6.9
Configuration	Mean displacement (mm)	Standard deviation (mm)	COV (%)
1	0.75	0.05	6.3
2	0.99	0.05	4.8
3	0.82	0.06	7.2

Compared to adhesive joint configuration 1, there is an increase of 37% in mean maximum load for configuration 2 and 45% for configuration 3. In terms of vertical displacement, we see that configuration 2 has a higher vertical deflection when the sample fails: 0.99 mm, while configuration 1 only has 0.75 mm deflection. We observe that as the length of the adhesive joint increases, the maximum load also increases.

As a measure to assess the stiffness of the bond, the ratio between the force build-up and the vertical displacement of the beam is calculated. This is always done in a zone where the curve showed a constant slope, between displacements of 0.3 mm and 0.6 mm. The diagram (see Fig. 7) shows that adhesive joint configuration 3 has the highest force build-up per millimetre vertical displacement (30.5 kN/mm), an increase of 8% compared to configuration 1 (28.2 kN/mm). Configuration 2 shows a stiffness of 24.7 kN/mm, which is 9% lower than configuration 1.

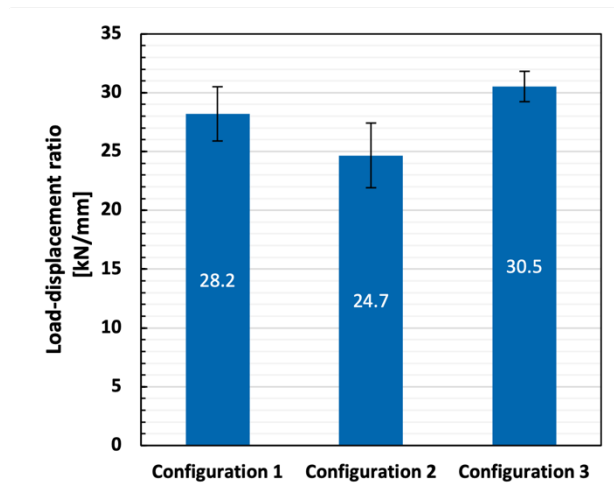


Fig. 7: Average load-displacement ratio.

The stress in the glass is calculated based on the standard for FRP composite bonded to concrete (ASTM D7958/D7958M). The method for FRP is slightly adapted to the use of glass.

$$F = \left(\frac{P}{2}\right) \left(\frac{1.5}{1 - \alpha/3}\right)$$

where:

F maximum force in glass, N

P maximum applied force indicated by testing machine, N

$$\alpha = \beta + \sqrt{\beta^2 + 2\beta} \leq 0.5$$

$$\beta = \frac{K^*w}{E_c bd}$$

where:

K* glass tensile stiffness per unit width, N/mm

b width of concrete test beam, mm

d overall depth of concrete test beam, mm

E_c modulus of elasticity of concrete, MPa (E_c = 4733√f_c)

With the values of F (maximum force in the glass), the stress in the glass can be calculated by dividing with the glass cross section (125 mm x 8 mm = 1000 mm²). The mean values of the stress in the glass of each adhesive joint configuration are shown in Fig. 8.

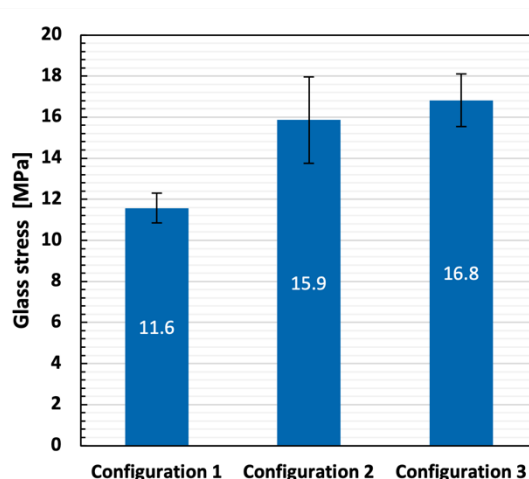


Fig. 8: Glass stress.

The calculated glass stresses always remain well under the characteristic tensile strength of basic soda lime silica glass (45 MPa). This was expected, as the glass never failed first.

The adhesive joint configuration seems to have an important impact on the stiffness of the element and the stress in the glass. To investigate the cause of this, it is interesting to examine the failure modes (see Fig. 9).

For configuration 1, a crack is forming parallel to the edge of the notch. This crack starts at the outer edge of the adhesive strip and follows a path of approximately 45° to the middle of the notch. Therefore, a piece of concrete in the shape of a triangular prism is breaking off. This was expected if the strength of the bond line is sufficiently high. Beams with adhesive configuration 2 show a different failure mode. Here, a thin layer of the concrete substrate is coming off. The failure mode of configuration 3 seems to be a mix of the previous failure modes. A thin layer of concrete detaches from the specimen, and close to the edge the corner of the concrete breaks off (see Fig. 10).

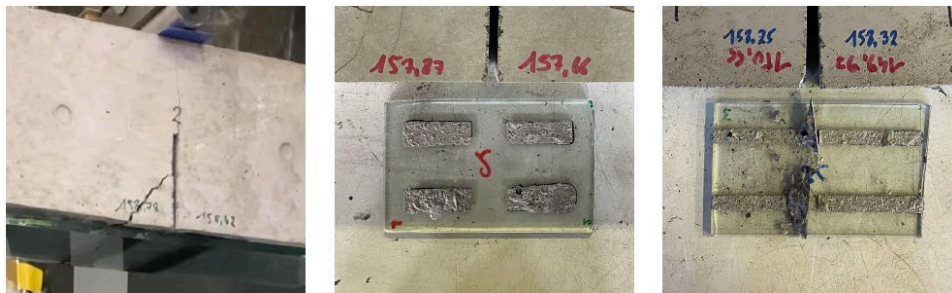


Fig. 9: Failure mode of a specimen with adhesive configuration 1 (left), 2 (middle) and 3 (right).



Fig. 10: Failure mode of a specimen with adhesive configuration 3.

3.2. Influence of adhesive type

Fig. 11 depicts the load-displacement curves of the four samples where different adhesives are used with the same adhesive joint configuration. The test result of each adhesive type is reported (see Table 3), followed by a discussion and reflection.

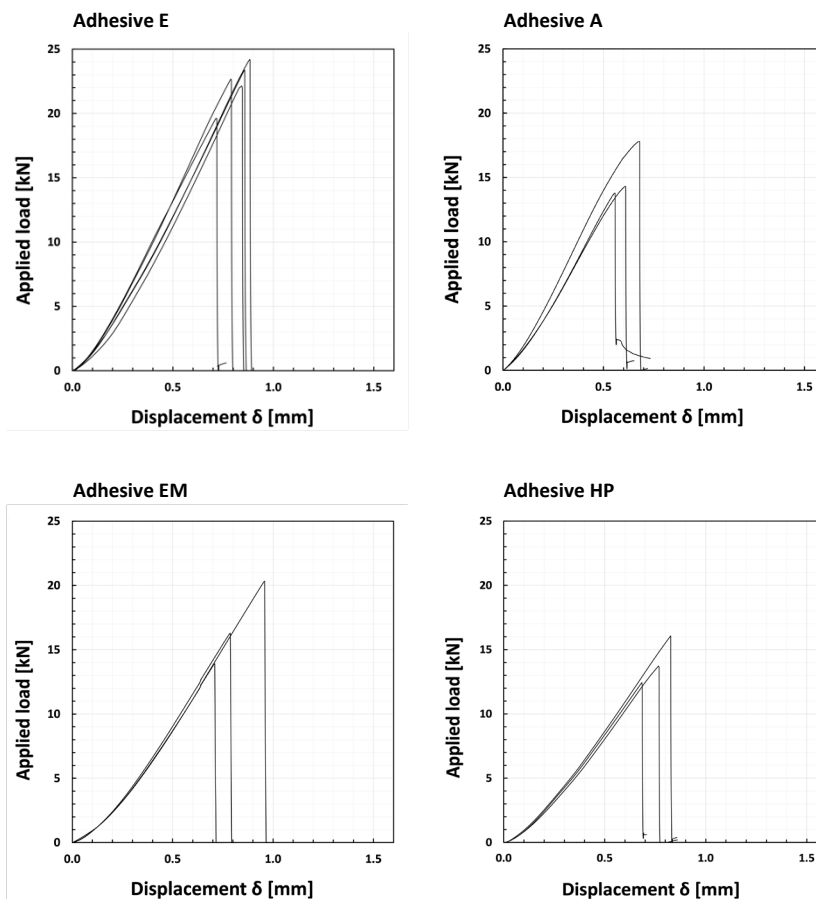


Fig. 11: Load-displacement curves the specimens with adhesive E, adhesive A, adhesive EM and adhesive HP.

Table 3: Summarising table of the test results.

Adhesive	Mean maximum load (kN)	Standard deviation (kN)	COV (%)
Adhesive E	22.4	1.6	6.9
Adhesive A	15.3	1.8	11.7
Adhesive EM	16.9	2.7	15.7
Adhesive HP	14.1	1.5	10.7
Adhesive	Mean displacement (mm)	Standard deviation (mm)	COV (%)
Adhesive E	0.82	0.06	7.2
Adhesive A	0.62	0.04	6.4
Adhesive EM	0.82	0.10	12.7
Adhesive HP	0.76	0.06	9.8

Adhesive E reached a mean maximum load of 22.4 kN. The other adhesives did not reach the same load before failure: they failed between 14 and 17 kN. Adhesive E and EM, both epoxy based, reach the highest mean maximum loads.

Again, the stiffness of the bond is expressed using the ratio between the force build-up and the vertical displacement (Fig. 12). Adhesive E gives the highest value with 30.5 kN/mm. Adhesive A has a slightly lower value of 29.3 kN/mm, which is 4% lower than adhesive E. Adhesive EM and adhesive HP show a load-displacement ratio of respectively 23.4 kN/mm (23% lower) and 20.9 kN/mm (31% lower).

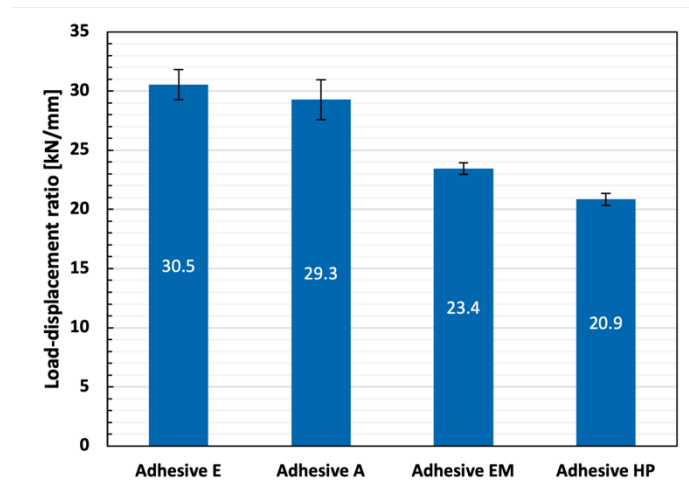


Fig. 12: load-displacement ratio.

Also, the stress in the glass is calculated (see Fig. 13), based on the standard for FRP composite bonded to concrete (ASTM D7958/D7958M).

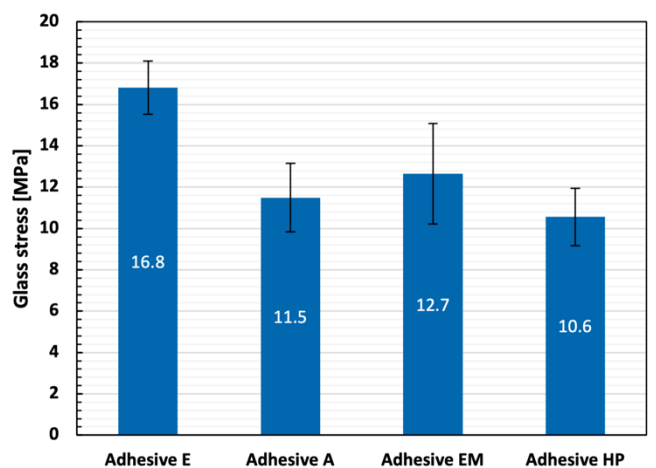


Fig. 13: Glass stress.

The calculated glass stresses always remain well under the tensile strength of basic soda lime silica glass. This was expected, as the glass never failed first.

For all adhesives similar failure modes are observed: a thin layer of the concrete substrate is delaminating. Also, at the edge of the notch, a piece of concrete is breaking off due to shear failure in the concrete. To increase the bond strength between the adhesive and the concrete, measures could be taken. It makes a difference if the adhesive bonds with concrete aggregates instead of only the top layer of the concrete element. Concrete surface preparation may increase the bond strength, as it increases surface roughness and exposes aggregates. This way, other failure modes can be obtained (Chen et al., 2019).

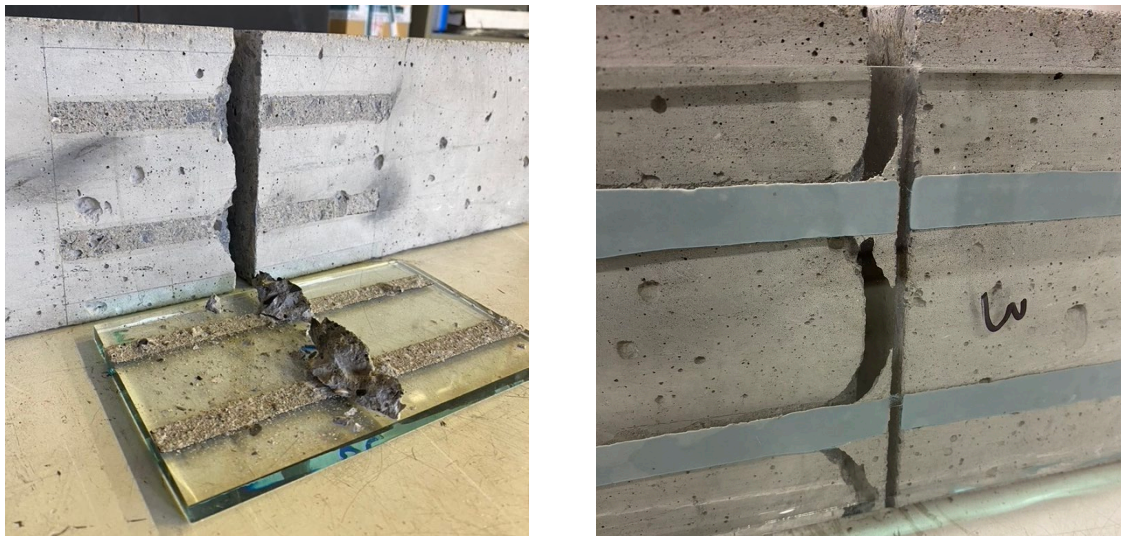


Fig. 14: Failure modes of adhesive E (left) and adhesive EM (right).

4. Conclusions

Previous tests investigated the bond behaviour of glass-concrete joints through three-point bending tests, varying in adhesive joint configuration and adhesive types.

Several key influencing factors can be identified. First, bonding close to the edge will result in concrete shear failure towards the edge, as expected. Second, failure generally occurs in the substrate layer of the concrete. Finally, the bond length influences the bond strength between the glass and the concrete.

The epoxy based adhesives seem to have the best bond between glass and concrete: these samples reached the highest mean maximum force. In terms of stiffness, the samples with the hybrid polymer-based adhesive reach the lowest values. Both adhesive E (epoxy based) and the adhesive A (acrylate based) perform similarly.

Moving forward, future research can delve into more realistic applications of glass adhesively bonded to concrete. Additionally, exploring the influence of other parameters, such as the type of glass (e.g., annealed float glass, laminated annealed float glass, laminated thermally toughened glass) and the use of concrete surface treatments (e.g., mechanical roughening, acid etching) can provide valuable insights into optimizing the structural performance of glass-concrete hybrid systems.

Acknowledgements

The authors acknowledge the support of fischerwerke GmbH & Co. KG.

References

- Achintha, M.: Sustainability of glass in construction. Elsevier eBooks (2016). <https://doi.org/10.1016/b978-0-08-100370-1.00005-6>
- ASTM International: Standard Test Method for Evaluation of Performance for FRP Composite Bonded to Concrete Substrate using Beam Test. D7958/D7958M.
- Centelles, X., Castro, J. R., & Cabeza, L. F. Experimental results of mechanical, adhesive, and laminated connections for laminated glass elements – A review. *Engineering Structures/Engineering Structures (Online)*, 180, 192–204 (2018). <https://doi.org/10.1016/j.engstruct.2018.11.029>
- CEN/TS 19100-1:2021. Design of glass structures - Part 1: Basis of design and materials.
- Chen, C., Li, X., Zhao, D., Huang, Z., Sui, L., Xing, F., & Zhou, Y.: Mechanism of surface preparation on FRP-Concrete bond performance: A quantitative study. *Composites Part B: Engineering* (2019). <https://doi.org/10.1016/j.compositesb.2018.11.027>
- Freytag, B. Glass-Concrete composite Technology. *Structural Engineering International* (2004). <https://doi.org/10.2749/101686604777963991>
- Harrison, E., Berenjian, A., & Seifan, M. Recycling of waste glass as aggregate in cement-based materials. *Environmental Science and Ecotechnology*, 4, 100064 (2020). <https://doi.org/10.1016/j.ese.2020.100064>
- Lee, H., & Cho, Y.: Evaluation of the mechanical properties of steel reinforcement embedded in concrete specimen as a function of the degree of reinforcement corrosion. *International Journal of Fracture* (2009). <https://doi.org/10.1007/s10704-009-9334-7>
- Narayanasamy, S., Yaragal, S., & Palanisamy, T. Environmental sustainability of waste glass as a valuable construction material – A critical review. *Ecology Environment and Conservation*. 24, 335–342 (2018)
- NBN EN 1992-1-1. Design of concrete structures - Part 1-1: General rules and rules for buildings.
- Popovici, I. C., & Lupascu, N. Chemical durability of soda-lime glass in aqueous acid solutions. *Comunicările Conferinței De Vibrații În Construcția De Mașini*. 23(1), 128–132 (2012). <https://doi.org/10.2478/v10310-012-0021-6>
- Serafinavičius, T., & Kvedaras, A. K. Challenges to Structural Glass: What have been Already Done? *Engineering Structures and Technologies*. 3(2), 79–89 (2011). <https://doi.org/10.3846/skt.2011.10>
- Sharma, N., Sharma, P., & Parashar, A. K. Use of waste glass and demolished brick as coarse aggregate in production of sustainable concrete. *Materials Today: Proceedings*, 62, 4030–4035 (2022). <https://doi.org/10.1016/j.matpr.2022.04.602>
- Tatar, J., & Milev, S.: Durability of Externally bonded Fiber-Reinforced polymer composites in concrete structures: A Critical review. *Polymers* (2021). <https://doi.org/10.3390/polym13050765>
- Udi, U. J., Yussof, M. M., Ayagi, K. M., Bedon, C., & Kamarudin, M. K. A. Environmental degradation of structural glass systems: A review of experimental research and main influencing parameters. *Ain Shams Engineering Journal*. 14(5), 101970 (2023). <https://doi.org/10.1016/j.asej.2022.101970>

Platinum Sponsor



Gold Sponsors



Silver Sponsors



Organising Partners

